

## FLUID FLOW AND GAS-LIQUID MASS TRANSFER IN GAS-INJECTED VESSEL

Shoji TANIGUCHI<sup>1</sup>, Seiji KAWAGUCHI<sup>2</sup> and Atsushi KIKUCHI<sup>1</sup>

<sup>1</sup> Department of Metallurgy, Graduate School of Engineering, Tohoku University, Sendai 980-8579, JAPAN

<sup>2</sup> Formerly Graduate School of Tohoku Univ. Now at NACHI FUJIKOSHI Corp., Toyama-pref. 930-0965, JAPAN

### ABSTRACT

Fluid flow, bubble distribution and gas-liquid mass transfer in a water model vessel with gas injection were analyzed to make clear the effect of turbulence on metallurgical reactions in ladles. Continuity equation, Navier-Stokes equation,  $k-\epsilon$  equation and bubble-dispersion equation in axially symmetrical form were solved numerically. Calculated time-averaged liquid velocities and fluctuating velocities agreed well with the measured results by a Laser-Doppler Velocimetry. Calculated local gas-holdup distribution also agreed with the observed results. Volumetric coefficients were estimated in two regions in the vessel, bubble-dispersion zone and free surface of liquid, based on the eddy-cell model using calculated results of  $\epsilon$ . The results were compared with the observed ones for CO<sub>2</sub>-water system obtained in our previous study. Estimated results gave a reasonable agreement only for the bubble-dispersion region. In the case of the volumetric coefficients at free surface, calculated results were larger than the observed ones. The reason of this disagreement was discussed based on the free surface fluctuation.

### INTRODUCTION

Gas injection into molten steel plays important roles in steelmaking processes. It realizes rapid mixing of molten metal, enhancement of refining reactions, and inclusion removal. In order to clarify these effects, phenomena of molten metal flow and mass transfer should be clearly understood. In recent years, a number of numerical and physical models have been applied to these subjects. Most of recent numerical simulations on the fluid flow under gas injection have been carried out by the use of the  $k-\epsilon$  model. To express the bubble-dispersion zone (BDZ), different approaches have been applied, (1) *single phase with variable density* (Mazumdar and Guthrie, 1985; Castillejos et al., 1989; Woo et al., 1990; Kikuchi, 1993; and Zhu et al., 1995) (2) *discrete bubbles in continuous phase (Lagrangian-Eulerian model)*, (Johansen and Boysan, 1986, 1988), (3) *two phases (Eulerian-Eulerian model)* (Sawada and Ohashi, 1987; Illegbusi and Szekely;

1990; Turkoglu and Farouk, 1991). Although the shape of BDZ should be given a-priori in the first model except our model (Kikuchi, 1993), it can be predicted theoretically in the latter two models.

Regarding mass-transfer model, the Danckwerts' surface-renewal model (Danckwerts, 1951) seems most adequate

compared with other models like the film model or Higbie's penetration model (Higbie, 1935), because it considers the random renewal of liquid surface due to turbulent eddies. However, only few works have been done until now, which apply the surface-renewal model to the mass-transfer analysis of gas-injection system taking into account of turbulence characteristics (Taniguchi et al., 1990).

The authors have made various studies on fluid flow and gas-liquid mass transfer, in which the bubble dispersion model has been applied (Taniguchi et al., 1988). This model belongs to the single-phase model combined with the bubble-diffusion equation for describing the shape and density distribution of BDZ. Experimental studies were also carried out by using CO<sub>2</sub>-water system, and volumetric coefficients in BDZ and at free surface were obtained separately (Bessho et al., 1985 and Taniguchi et al., 1990). In the present study, these coefficients have been analyzed by a hybrid model of our bubble-dispersion model and the eddy-cell model derived from the surface-renewal model.

### OUTLINE OF MODELS

#### Flow Model

Equations of continuity, motion and bubble dispersion used in the present study are shown as follows:

$$\frac{1}{r} \frac{\partial}{\partial r} (\rho r u) + \frac{\partial}{\partial z} (\rho v) = 0 \quad (1)$$

$$\rho \left( u \frac{\partial u}{\partial r} + v \frac{\partial u}{\partial z} \right) = -\frac{\partial p}{\partial r} + \frac{1}{r} \frac{\partial}{\partial r} \left[ \rho v_e r \left( 2 \frac{\partial u}{\partial r} - \frac{2}{3} \vec{\nabla} \cdot \vec{v} \right) \right] + \frac{\partial}{\partial z} \left[ \rho v_e \left( \frac{\partial v}{\partial r} + \frac{\partial u}{\partial z} \right) \right] - \frac{\rho v_e}{r} \left( \frac{2}{r} u - \frac{2}{3} \vec{\nabla} \cdot \vec{v} \right) \quad (2)$$

$$\rho \left( u \frac{\partial v}{\partial r} + v \frac{\partial v}{\partial z} \right) = -\frac{\partial p}{\partial z} + \frac{1}{r} \frac{\partial}{\partial r} \left[ \rho v_e r \left( \frac{\partial v}{\partial r} + \frac{\partial u}{\partial z} \right) \right] + \frac{\partial}{\partial z} \left[ \rho v_e \left( 2 \frac{\partial v}{\partial z} - \frac{2}{3} \vec{\nabla} \cdot \vec{v} \right) \right] + \rho_L \sigma g \quad (3)$$

$$u \frac{\partial \sigma}{\partial r} + (v + v_B) \frac{\partial \sigma}{\partial z} = \frac{1}{r} \frac{\partial}{\partial r} \left( r D_e \frac{\partial \sigma}{\partial r} \right) + \frac{\partial}{\partial z} \left( D_e \frac{\partial \sigma}{\partial z} \right) \quad (4)$$

where  $u$  and  $v$  are the time-averaged liquid velocities in  $r$  and  $z$  direction,  $\sigma$  local gas holdup,  $\rho$  density of gas-liquid mixture,  $\rho_L$  liquid density. Boundary conditions are as follows:

$$r = 0, 0 < z < z_1 : u = \partial v / \partial r = \partial \sigma / \partial r = 0 \quad (5)$$

$$r = r_1, 0 < z < z_1 : u = v = \partial\sigma / \partial r = 0 \quad (6)$$

$$z = 0, 0 < r < r_c : u = v = 0, \sigma = 1 \quad (7)$$

$$z = 0, r_c < r < r_1 : u = v = \sigma = 0 \quad (8)$$

$$z = z_1, 0 < r < r_1 : \partial u / \partial z = v = \partial\sigma / \partial z = 0 \quad (9)$$

where

$$r_c = \sqrt{q_G / \pi v_B}, \quad \rho = (1 - \sigma)\rho_L \quad (10)$$

The effective diffusivity of bubbles,  $D_e$ , was assumed to be equal to the effective kinematic viscosity,  $\nu_e$ . The terminal velocity of bubble,  $v_B$ , and mean bubble diameter,  $d_B$ , were estimated by the empirical equation of Tadaki and Maeda (1961, 1963).

Equations of  $k$  and  $\varepsilon$  are shown as follows:

$$\begin{aligned} \frac{1}{r} \frac{\partial}{\partial r} (\rho r u k) + \frac{\partial}{\partial z} (\rho v k) &= \frac{1}{r} \frac{\partial}{\partial r} \left( \rho r \frac{v_e}{\sigma_k} \frac{\partial k}{\partial r} \right) \\ &+ \frac{\partial}{\partial z} \left( \rho \frac{v_e}{\sigma_k} \frac{\partial k}{\partial z} \right) + (G + G_B) - \rho \varepsilon \end{aligned} \quad (11)$$

$$\begin{aligned} \frac{1}{r} \frac{\partial}{\partial r} (\rho r u \varepsilon) + \frac{\partial}{\partial z} (\rho v \varepsilon) &= \frac{1}{r} \frac{\partial}{\partial r} \left( \rho r \frac{v_e}{\sigma_\varepsilon} \frac{\partial \varepsilon}{\partial r} \right) \\ &+ \frac{\partial}{\partial z} \left( \rho \frac{v_e}{\sigma_\varepsilon} \frac{\partial \varepsilon}{\partial z} \right) + \frac{c_1}{k} \varepsilon (G + G_B) - \frac{c_2}{k} \rho \varepsilon^2 \end{aligned} \quad (12)$$

where  $G$  and  $G_B$  are the generation term of turbulence due to velocity gradient and slip motion of bubbles.

$$\begin{aligned} G &= \mu_t \left[ 2 \left[ \left( \frac{\partial u}{\partial r} \right)^2 + \left( \frac{\partial v}{\partial z} \right)^2 + \left( \frac{u}{r} \right)^2 \right] + \left( \frac{\partial v}{\partial r} + \frac{\partial u}{\partial z} \right)^2 \right] \\ &- \frac{2}{3} \mu_t (\vec{\nabla} \cdot \vec{v})^2 \end{aligned} \quad (13)$$

$$G_B = \rho_L \sigma g v_B \quad (14)$$

Eq.(14) was applied to gas-injection system by Johansen and Boysan (1988). Effective kinematic viscosity,  $\nu_e$ , is obtained by,

$$\nu_e = \mu_e / \rho, \quad \mu_e = \mu + \mu_t, \quad \mu_t = \rho C_D k^2 / \varepsilon \quad (15)$$

The following values were adopted as the constants included in  $k$ - $\varepsilon$  equations.

$$C_D = 0.09, C_1 = 1.44, C_2 = 1.92, \sigma_k = 1.0, \sigma_\varepsilon = 1.3$$

Boundary conditions for  $k$ - $\varepsilon$  equations are given by,

$$r = 0, 0 < z < z_1 : \partial k / \partial r = \partial \varepsilon / \partial r = 0 \quad (16)$$

$$r = r_1, 0 < z < z_1 : k = \varepsilon = 0 \quad (17)$$

$$z = 0, 0 < r < r_1 : k = \varepsilon = 0 \quad (18)$$

$$z = z_1, 0 < r < r_1 : \partial k / \partial z = \partial \varepsilon / \partial z = 0 \quad (19)$$

Wall function was adopted at grid points adjacent to solid walls. All equations depicted above were transformed into dimensionless form, and the stream function ( $\psi$ ) and vorticity ( $\zeta$ ) defined by the following equations were introduced.

$$U = \frac{1}{R\delta} \frac{\partial \psi}{\partial z}, \quad V = -\frac{1}{R\delta} \frac{\partial \psi}{\partial R} \quad (20)$$

$$\zeta = \frac{1}{R} \left( \frac{\partial U}{\partial Z} - \frac{\partial V}{\partial R} \right) \quad (21)$$

where

$$U = r_1 u / v, \quad V = r_1 v / v, \quad R = r / r_1, \quad Z = z / r_1, \quad \delta = \rho / \rho_L.$$

The upwind difference scheme was applied and successive over-relaxation method was used for solving the finite difference equations. The present code was developed by the authors and was restricted to 2D axially symmetrical system because the stream function was introduced. This code was checked preliminary for round pipe flows.

### Mass Transfer Model

Kataoka and Miyauchi (1969) derived Eq.(22) based on the assumption that the surface renewal should be made by the smallest eddy having the highest renewal frequency.

$$k_L = 0.5(\varepsilon / \nu)^{1/4} D^{1/2} \quad (22)$$

where  $D$  is the diffusivity of solute. They indicated that this equation applied well to the CO<sub>2</sub> absorption into water across a turbulently agitated free surface. Lamont and Scott (1970) derived similar equation as Eq.(22) by assuming that every eddies in the inertial sub-range of turbulence contributed to the surface renewal. Although they did not give the constant, 0.5, in Eq.(22), their model is thought to be more advanced than Kataoka and Miyauchi's model, because they took into account of the size distribution of eddies.

The volumetric coefficient,  $k_L A$  in BDZ, where  $A$  is the gas-liquid interfacial area, was estimated as follows: the local mass-transfer coefficient,  $k_{LB}$  was calculated from Eq.(22) by substituting the computed result of  $\varepsilon$ , and multiplying the local specific area of bubble,  $(6/d_B)\sigma$ . Local volumetric coefficient derived by the above procedure was then integrated throughout the vessel and  $(k_L A)_B$  was obtained. If the increase in free surface area is negligible, the volumetric coefficient at the free surface,  $(k_L A)_S$ , can be obtained by Eq.(22) substituting the computed result of average energy dissipation rate at the free surface and multiplying flat surface area,  $\pi r_1^2$ .

For comparison, Higbie's penetration model was also applied. The mass-transfer coefficient of this model is expressed by,

$$k_L = 2\sqrt{D/\pi\tau} \quad (23)$$

The residence time of liquid element on bubble surface and free surface are calculated by the following equations:

$$\tau_B = d_B / v_B \quad (24), \quad \tau_S = r_1 / u_S \quad (25)$$

where  $u_S$  is the average radial velocity of free surface obtained by the tracer method. The value of  $(k_L A)_B$  was obtained by multiplying  $k_{LB}$  by average specific surface area of bubble,  $(6/d_B)\bar{\sigma} V$ , where  $V$  is the volume of fluid. The value of  $(k_L A)_S$  was obtained by  $k_{LS} \pi r_1^2$ .

### EXPERIMENTAL

Measurements of velocity field, volumetric coefficient and free surface fluctuation were carried out in a water vessel with 0.145m radius and 0.2m water height. Nitrogen was injected into water through a 6mm-diameter nozzle located at the bottom center of the vessel. Gas-flow rate was changed from 16.7 to 167x10<sup>-6</sup>m<sup>3</sup>s<sup>-1</sup>.

The radial components of time-averaged velocity and r.m.s. of the fluctuating velocity were measured by the use of Laser Doppler Velocimetry (LDV).

Volumetric coefficient,  $k_L A$ , was measured by using CO<sub>2</sub>-water system in the previous paper (Taniguchi et al., 1990). The definition of  $k_L A$  is given by,

$$dC/dt = (k_L A/V)(C_e - C) \quad (26)$$

where  $C_e$  is the equilibrium concentration of CO<sub>2</sub> in water. This coefficient is composed of two coefficients, in BDZ and at free surface as follows:

$$k_L A = (k_L A)_B + (k_L A)_S \quad (27)$$

In the previous study, these two coefficients were separated from  $k_L A$  experimentally.

The shape and fluctuation of the free surface were measured to obtain the surface area and oscillating velocity of free surface which are closely related to the characteristic of mass transfer across the free surface. In the experiment radial profiles of free surface illuminated by a light sheet were recorded by a video camera during 10 s, and each profile at every 1/30 s was processed to obtain the average shape, amplitude of fluctuation, and r.m.s. of the fluctuating velocity.

## RESULTS AND DISCUSSION

### Fluid Flow and Bubble Dispersion

Figure 1 shows a visualized flow pattern obtained by a tracer method. There can be seen a large clockwise recirculating flow near the side wall and a stagnant region near the bottom. The width of BDZ becomes large with increasing  $z$ .

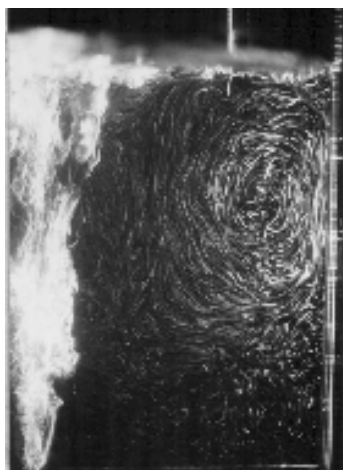
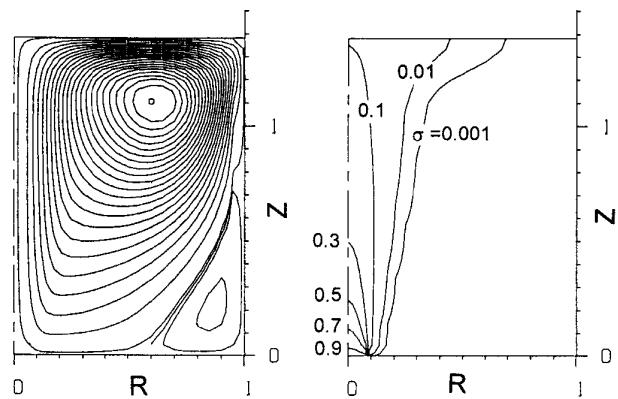


Figure 1: Visualize flow pattern ( $q_G=83.3 \times 10^{-6} \text{m}^3 \text{s}^{-1}$ ).

(a) Stream line pattern      (b) Local gas holdup

Figure 2: Computed results of stream line pattern and



local gas holdup at  $q_G=83.3 \times 10^{-6} \text{m}^3 \text{s}^{-1}$ .

The computed flow pattern and local gas holdup distribution are shown in Fig.2(a) and (b), respectively, at the same condition as Fig.1. The features of the flow and BDZ are simulated well by the numerical calculation. Figure 3 shows the computed effective kinematic viscosity,  $\nu_e$  (cm<sup>2</sup>/s). The value of  $\nu_e$  attains maximum at the center of the free surface where bubbles go out.

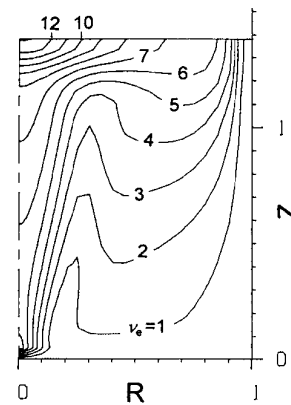
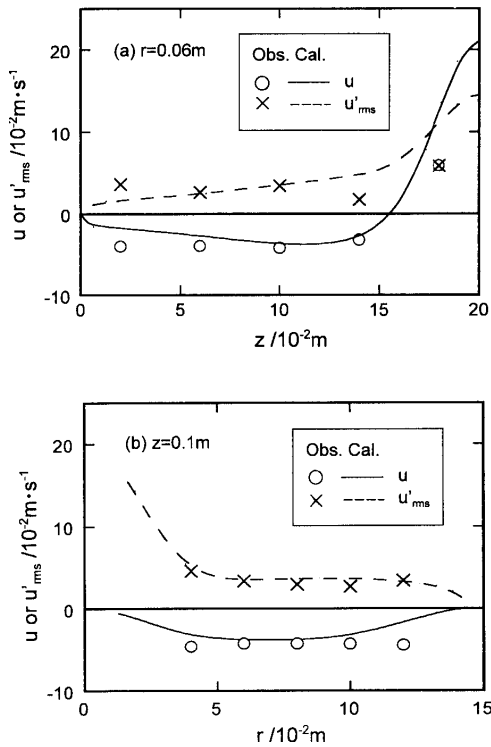
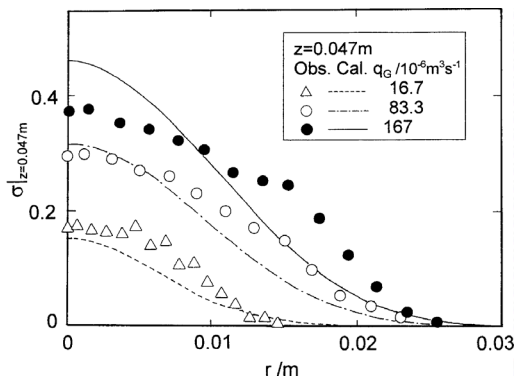


Figure 3: Computed effective kinematic viscosity at  $q_G=83.3 \times 10^{-6} \text{m}^3 \text{s}^{-1}$ .



**Figure 4:** Comparison between calculated and measured velocities at  $q_G = 83.3 \times 10^{-6} \text{ m}^3 \text{ s}^{-1}$ .

The radial velocity components obtained by LDV at bubble-free zone are compared with the numerical calculation in Fig.4. Not only the time-averaged radial velocities but also r.m.s. of the fluctuating velocities are roughly simulated by the calculation. Comparison of calculated local gas-holdup distribution with observed results reported by Taniguchi et al. (1988) is shown in Fig.5. There can be seen reasonable agreement between calculated and observed local gas-holdup distribution at different gas-flow rates.



**Figure 5:** Comparison between calculated and measured gas-holdup distribution. Measurement was made by the electrical resistance probe.

### Mass transfer

Volumetric coefficients in BDZ estimated by the eddy-cell model and penetration model are shown in Fig.6 comparing with the observed results.

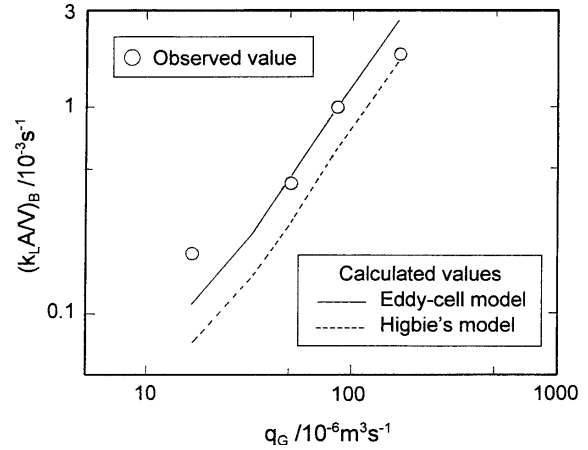


**Figure 6:** Comparison between calculated and observed volumetric coefficients in BDZ.

The observed results are estimated well by the eddy-cell model. Despite the high intensity of turbulence in BDZ, it is found that the penetration model also gives fairly good estimation. This may be attributable to the high surface renewal rate indicated by Eq.(24) due to large slip velocity of bubbles. Volumetric coefficient at free surface is then discussed. First, mean area of the free surface was calculated from the observed surface profiles assuming axially symmetrical shape. As a result, the area was found to increase only 10% even at the largest gas-flow rate. Therefore, the calculated mass transfer coefficients were directly compared with the observed ones neglecting the change in surface area. Figure 7 shows the comparisons of measured values of  $k_{LS}$  with the predictions by the two models. It is seen from the figure that the eddy-cell model gives larger values and the penetration model gives smaller values than the observed  $k_{LS}$ . The dependence of observed  $k_{LS}$  on  $q_G$  is larger than that of the eddy-cell model, and is very weak for the penetration model. The observed value of  $k_{LS}$  is close to the penetration model at low gas-flow rate and approaches the eddy-cell model at high gas-flow rate. In order to discuss the reason why the eddy-cell model failed to estimate  $k_{LS}$ , the free surface fluctuation was investigated.

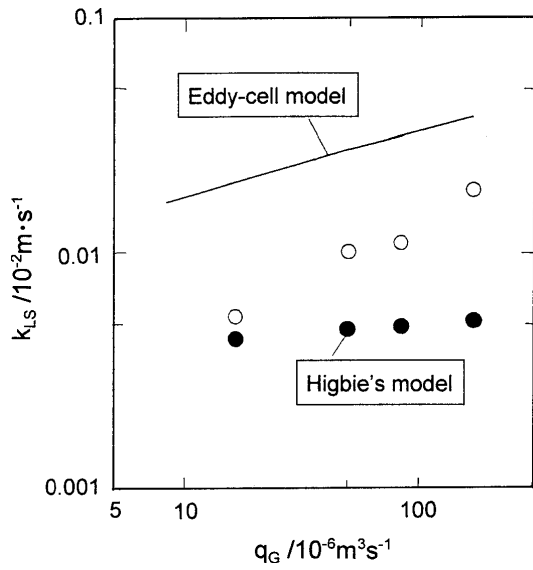


**Figure 7:** Comparison between calculated and observed mass-transfer coefficients at free surface.

Figures 8.(a) and (b) give the mean shapes of the free surface and amplitudes of oscillation at different gas-flow rates. There can be seen two peaks in the amplitude close to the center. This is attributable to the swirling of bubble plume.

Comparisons were made in Fig.9 between observed surface fluctuating velocities and calculated r.m.s. values of vertical component of turbulent velocity at the free surface,  $((2/3)k_{z=z1})^{1/2}$ . There is reasonable agreement between observed and calculated fluctuating velocities at any gas-flow rates. This indicates that the surface wave is mainly generated by the turbulence at the free surface and the fluid flow is fully developed turbulence even at the smallest gas-flow rate in the present condition. Considering that energy is needed for keeping steady fluctuating motion of free surface, a part of the stirring power introduced into the system should be consumed there. The energy-dissipation rate delivered to the oscillating motion of the free surface can be estimated by Eq.(28) and (29), by assuming that the amplitude of oscillation corresponds with the scale of turbulent eddy (Johansen et al. 1986) at the free surface.

$$\Lambda = 2A = C_D^{3/4} k^{3/2} / \varepsilon \quad (28)$$

$$\therefore \varepsilon_{sw} = \frac{C_D^{3/4}}{2A} \left( \frac{3}{2} v_{rms}^2 \right)^{3/2} = 0.151 \cdot v_{rms}^3 / A \quad (29)$$

Substituting observed value of  $v'_{rms}$  and  $A$  into Eq. (29), and averaging over the free surface, the value of  $\bar{\varepsilon}_{sw}$  was calculated. The results are shown in Table 1 with the values obtained from the result of flow simulation,  $\bar{\varepsilon}_s$ .

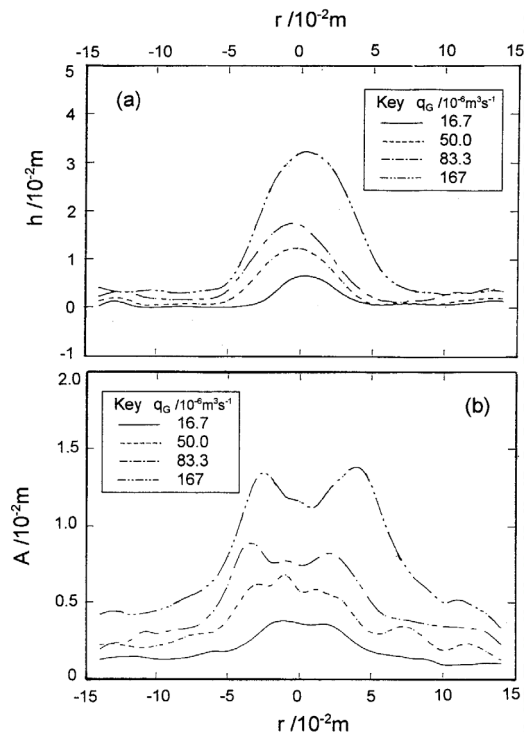


**Figure 8:** Observed shapes and amplitudes of oscillation of free surface.

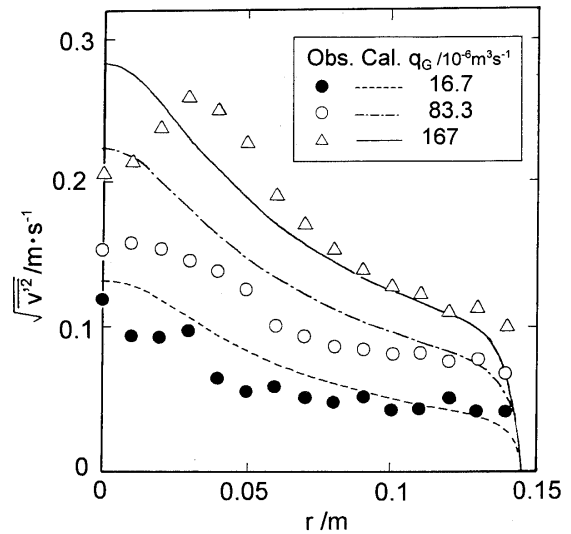


**Figure 9:** Comparison between calculated and observed oscillation velocities of free surface.

**Table 1:** Values of  $\varepsilon$  at free surface.

$q_G / 10^{-6} \text{m}^3 \text{s}^{-1}$	$\bar{\varepsilon}_s / 10^{-4} \text{m}^2 \text{s}^{-3}$	$\bar{\varepsilon}_{sw}$	$\bar{\varepsilon}_s - \bar{\varepsilon}_{sw}$
16.7	87	144	-57
50.0	309	182	127
83.3	536	294	242
167	1137	817	320

It is found from the table that the value of  $\bar{\varepsilon}_{sw}$  is comparable to the value of  $\bar{\varepsilon}_s$ , which indicates that suitable amount of energy dissipation rate is consumed by the wave motion. If the value of  $\bar{\varepsilon}_s - \bar{\varepsilon}_{sw}$  is used for the surface renewal, it is thought that the surface renewal by turbulent eddy does not occur at the smallest gas-flow rate. However, surface renewal takes place at larger gas-flow rate and is promoted with increasing gas-flow rate. This hypothesis can explain well the results in Fig.7, however, further study should be needed for more clear understanding of the relationship between surface wave and turbulent mass transfer.

## CONCLUSION

The fluid flow and mass transfer in gas-injected vessel were investigated by numerical simulation and water-model experiments. A mathematical model composed of  $k$ - $\varepsilon$  model and bubble-dispersion model was applied. Flow pattern, gas-holdup distribution, velocities,  $k$  and  $\varepsilon$  distributions were calculated and a part of these results were found to agree with the observed results obtained by LDV and with the previous values of local gas-holdup. The volumetric coefficients in BDZ and at free surface were estimated by the eddy-cell model and Higbie's penetration model. Estimated value by the eddy-cell model agreed well with the observed results in BDZ, however it gave a larger value than the measured result at free surface. This discrepancy was explained by the wave motion of free surface which consumes a part of energy dissipation rate needed for surface renewal.

## REFERENCES

- MAZUMDAR, D. and GUTHRIE, R.I.L., (1985), "Hydro-dynamic Modeling of Some Gas Injection Procedures in Ladle Metallurgy Operations", *Metall. Trans. B*, **16B**, 83-90.
- BESSHO, N., TANIGUCHI, S. and KIKUCHI, A., (1985), "Mass Transfer between Gas and Liquid in a Gas-stirred Vessel", *Tetsu-to-Hagane*, **71**, 1623-1630.
- CASTILLEJOS, A.H., SALCADEAN, M.E. and BRIMACOMBE, J.K., (1989), "Fluid Flow and Bath Temperature Destratification in Gas-Stirred Ladles", *Metall. Trans. B*, **20B**, 603-611.
- WOO, J.S., SZEKELY, J., CASTILLEJOS, A.H., and BRIMACOMBE, J.K., (1990), "A Study on the Mathematical Modeling of Turbulent Recirculating Flows in Gas-Stirred Ladles", *Metall., Trans. B*, **21B**, 269-277.
- KIKUCHI, A., (1993), "Simulation of Fluid Flow in a Gas-injected System of Steelmaking Process", *Computer Aided Innovation of New Materials II*, ed. Doyama, M. et

al., Elsevier, 1707-1712.

ZHU, M., INOMOTO, T., SAWADA, I., and HSIAO, T., (1995), "Fluid Flow and Mixing Phenomena in the Ladle Stirred by Argon through Multi-tuyere", *ISIJ Int.*, **35**, 472-478.

JOHANSEN, S.T., BOYSAN, F. and ENGH, T.A., (1986), "Numerical Calculation of Removal of Inclusions and Dissolution of Refractory in a Bubble Stirred Ladle", *The 4th Japan-Nordic Countries Joint Symp on Science and Technology of Process Metallurgy, ISIJ*, 182-215.

JOHANSEN, S.T. and BOYSAN, F., (1988), "Fluid Dynamics in Bubble Stirred Ladles. Part II Mathematical Modeling", *Metall. Trans. B*, **19B**, 755-764.

SAWADA, I. and OHASHI, T., (1987), "Numerical Analysis of the Two Phase Flow in the Bottom-gas Blowing Ladle", *Tetsu-to-Hagane*, **73**, 669-676.

ILLEGBUSI, O.J. and SZEKELY, J., (1990), "The Modeling of Gas-bubble Driven Circulations Systems", *ISIJ Int.*, **30**, 731-739.

TUKOGLU, H. and FAROUK, B., (1990), "Numerical Computation of Fluid Flow and Heat Transfer in a Gas-Stirred Liquid Bath", *Metall. Trans. B*, **21B**, 771-781.

TANIGUCHI, S., KIKUCHI, A., MATSUZAKI, H., and BESSHO, N., (1988), "Dispersion of Bubbles and Gas-Liquid Mass Transfer in a Gas-Stirred System", *ISIJ Int.*, **28**, 262-270.

TANIGUCHI, S., OKADA, Y., SAKAI, A., and KIKUCHI, A., (1990), "Characteristics of Mass Transfer at the Free Surface of Liquid in a Gas-Stirred System", *Proc. 6th Int. Iron and Steel Congress, Nagoya, Japan*, **1**, 394-401.

DANCKWERTS, P.V., (1951), "Significance of Liquid-Film Coefficients in Gas Absorption", *Ind. Eng. Chem.*, **43**, 1460-1467.

HIGBIE, R., (1935), "The Rate of Absorption of a Pure Gas into a Still Liquid During Short Periods of exposure", *Trans. Am. Inst. Chem. Engrs.*, **35**, 365-389.

KATAOKA, H. and MIYAUCHI, T., (1969), "Gas Absorption into the Free Liquid Surface of Water Tunnel in Turbulent Region", *Kagaku-Kogaku*, **33**, 181-186.

LAMONT, J.C. and SCOTT, D.S., (1970), "An Eddy Cell Model of Mass Transfer into the Surface of a Turbulent Liquid", *AIChE J.*, **16**, 513-519.

TADAKI, T. and MAEDA, S., (1961), "On the Shape and Velocity of Single Air Bubbles Rising in Various Liquids", *Kagaku-Kogaku*, **25**, 254-263.

TADAKI, T. and MAEDA, S., (1963), "The Size of Bubbles from Single Orifices", *Kagaku-Kogaku*, **27**, 147-155.